

REPORT DOCUMENTATION PAGE			Form Approved OMB NO. 0704-0188	
Public Reporting burden for this collection of information is estimated to average 1 hour per response, including the time for reviewing instructions, searching existing data sources, gathering and maintaining the data needed, and completing and reviewing the collection of information. Send comment regarding this burden estimates or any other aspect of this collection of information, including suggestions for reducing this burden, to Washington Headquarters Services, Directorate for Information Operations and Reports, 1215 Jefferson Davis Highway, Suite 1204, Arlington, VA 22202-4302, and to the Office of Management and Budget, Paperwork Reduction Project (0704-0188), Washington, DC 20503.				
1. AGENCY USE ONLY (Leave Blank)		2. REPORT DATE 1 March 2007		3. REPORT TYPE AND DATES COVERED Final Report 01 Mar 05 - 30 Nov 06
4. TITLE AND SUBTITLE Semiconducting Nanocrystals in Mesostructured Thin Films for Optical and Opto-Electronic Device Applications			5. FUNDING NUMBERS  <b>Grant W911NF-05-1-0085</b>	
6. AUTHOR(S) Bradley F. Chmelka (Principal Investigator)				
7. PERFORMING ORGANIZATION NAME(S) AND ADDRESS(ES) Department of Chemical Engineering, University of California, Santa Barbara, Santa Barbara, California, 93106 USA			8. PERFORMING ORGANIZATION REPORT NUMBER	
9. SPONSORING / MONITORING AGENCY NAME(S) AND ADDRESS(ES) U. S. Army Research Office P.O. Box 12211 Research Triangle Park, NC 27709-2211			10. SPONSORING / MONITORING AGENCY REPORT NUMBER 48130.1-CH	
11. SUPPLEMENTARY NOTES The views, opinions and/or findings contained in this report are those of the author(s) and should not be construed as an official Department of the Army position, policy or decision, unless so designated by other documentation.				
12 a. DISTRIBUTION / AVAILABILITY STATEMENT Approved for public release; distribution unlimited.			12 b. DISTRIBUTION CODE	
13. ABSTRACT (Maximum 200 words)  The compositions, structures, and surface properties of InGaP, GaN, ZnSe, ZnS <sub>2</sub> , and SiO <sub>2</sub> nanocrystals and conjugated polymer/(SnS <sub>2</sub> or SiO <sub>2</sub> ) nanocomposite films have been measured and controlled to modify, enhance, and understand their optical and/or semiconducting properties over a hierarchy of dimensions, from molecular to macroscopic. This progress has enabled new and general strategies for the development and optimization of nanocrystals and nanostructured composites for applications in electro- or photoluminescent devices, sensors, and solid-state lighting.  The macroscopic optical and semiconducting properties of novel inorganic-organic hybrid materials, based on monodisperse nanocrystals and/or ordered nanostructured inorganic-organic composite solids with tunable compositions and dimensions, depend crucially on molecular-level compositions, structures, and interfaces. Till now, such molecular-level structural details have not been measured, not understood, nor have they been used as feedback criteria for improving or optimizing materials syntheses, or device processing conditions. During the course of this project, new molecular-level insights provided by very-high-field and multidimensional NMR characterization protocols have enabled the development of novel nano- and hierarchically scaled optical and semiconducting materials and devices. New and general strategies for controlling nanocrystal structures and interfaces have allowed the incorporation of semiconducting nanocrystals and polymers into nanocomposite films, yielding novel opto-electronic and optical properties.				
14. SUBJECT TERMS nanocrystals, semiconductors, optical materials, solid-state lighting, inorganic mesostructures, InGaP, GaN, ZnSe, ZnS, SiO <sub>2</sub> , Zn <sub>2</sub> TiO <sub>4</sub> , TiO <sub>2</sub> , SnS <sub>2</sub> , conjugated polymers, MEH-PPV, polyfluorene, surfactant/block-copolymer template species			15. NUMBER OF PAGES  16	
			16. PRICE CODE	
7. SECURITY CLASSIFICATION OR REPORT <b>UNCLASSIFIED</b>	18. SECURITY CLASSIFICATION ON THIS PAGE <b>UNCLASSIFIED</b>	19. SECURITY CLASSIFICATION OF ABSTRACT <b>UNCLASSIFIED</b>	20. LIMITATION OF ABSTRACT  <b>UL</b>	

NSN 7540-01-280-5500

298 (Rev.2-89)

Prescribed by ANSI Std. Z39-18

Standard Form

298-102

## Final Progress Report

# Semiconducting Nanocrystals in Mesostructured Thin Films for Optical and Opto-Electronic Device Applications

Bradley F. Chmelka (Principal Investigator)

USARO Grant W911NF-05-1-0085

### Foreword/Summary

The compositions, structures, and surface properties of InGaP, GaN, ZnSe, ZnS, ZnO, and SiO<sub>2</sub> nanocrystals and conjugated polymer/(SnS<sub>2</sub> or SiO<sub>2</sub>) nanocomposites have been measured and controlled to modify, enhance, and understand their optical and semiconducting properties over a hierarchy of dimensions, from molecular to macroscopic. This progress has enabled new opportunities for the development and optimization of nanocrystals and nanostructured composites for applications in electro- or photoluminescent devices, sensors, and solid-state lighting.

The objectives of this project have been the design, synthesis, processing, and characterization of optically responsive semiconducting nanocrystals and nanocomposites with tunable properties and their integration into devices. **We have shown that the macroscopic optical and semiconducting properties of novel inorganic-organic hybrid materials based on monodisperse nanocrystals and/or ordered nanostructured inorganic-organic composite solids with tunable compositions and dimensions, depend crucially on molecular-level compositions, structures, and interfaces.** Till now, such molecular-level structural details have not been measured, not understood, nor have they been used as feedback criteria for improving or optimizing materials synthesis or device processing conditions. During the course of this project, progress in the development of new very-high-field and multidimensional NMR characterization protocols have underpinned progress in the development of new synthesis/processing protocols for improving optical and semiconducting materials and devices. **New and general strategies for controlling nanocrystal structures and interfaces have allowed the incorporation of semiconducting nanocrystals and polymers into nanocomposite films, yielding novel opto-electronic and optical properties.**

## Table of Contents

<b>List of Figures.....</b>	<b>6</b>
<b>Statement of the Problem.....</b>	<b>7</b>
<b>Summary of the Most Important Results .....</b>	<b>7</b>
<b>Indium gallium phosphide (InGaP) nanocrystals.....</b>	<b>7</b>
<b>ZnSe and ZnS nanowires and nanorods, ZnO.....</b>	<b>9</b>
<b>Conjugated polymers in nanostructured composite materials.....</b>	<b>10</b>
<b>List of Publications and Meetings/Seminars/Conferences.....</b>	<b>11</b>
<b>Papers published in peer-reviewed journals.....</b>	<b>11</b>
<b>Manuscripts submitted and in preparation, but not yet published.....</b>	<b>11</b>
<b>Invited Lectures.....</b>	<b>12</b>
<b>Awards .....</b>	<b>12</b>
<b>Invention disclosures, patents applied for and awarded .....</b>	<b>12</b>
<b>Transfer of materials or techniques to Army, DoD, or industry .....</b>	<b>13</b>
<b>Value of this program to the Army.....</b>	<b>13</b>
<b>List of Participating Scientific Personnel.....</b>	<b>13</b>

## List of Figures

<b>Figure 1:</b> TEM of 4.5 nm InGaP nanocrystal.....	14
<b>Figure 2:</b> $^{71}\text{Ga}$ NMR spectra at 19 T of as-synthesized and etched InGaP nanocrystals.....	14
<b>Figure 3:</b> $^{115}\text{In}$ NMR spectra at 19 T of as-synthesized and etched InGaP nanocrystals.....	14
<b>Figure 4:</b> 2D double-quantum $^{31}\text{P}$ NMR spectrum, 4.5 nm InGaP nanocrystals.....	15
<b>Figure 5:</b> TEM of of 10 nm, 5 nm, 1.5 nm ZnSe nanocrystals .....	16
<b>Figure 6:</b> $^{77}\text{Se}$ and $^{67}\text{Zn}$ NMR spectra of 10 nm, 5 nm, 1.5 nm ZnSe nanocrystals.....	16
<b>Figure 7:</b> SEM and HR-TEM images, SAXS of vertically aligned nanocomposite silica .....	17
<b>Figure 8:</b> PF8-SnS <sub>2</sub> nanocomposite and device, 2D $^{119}\text{Sn}\{^1\text{H}\}$ HETCOR NMR spectrum....	18

## Statement of the Problem

With the support of USARO grant **W911NF-05-1-0085**, we have developed, tested, and refined our hypotheses:

- (1) that local compositional and structural heterogeneities at inorganic-organic interfaces play governing roles in establishing macroscopic optical properties of semiconductor nanocrystals and nanocomposites;
- (2) that identifying the molecular natures of such heterogeneities would allow us to correlate and control key compositional and structural features of the materials with synthesis and processing conditions, and
- (3) that the optimization of inorganic-organic interface compositions and compositions would yield improved material and device performances, with respect to different optical or semiconducting property criteria.

Close feedback between new molecular-level NMR characterization insights and synthesis and processing protocols have allowed each of these hypotheses to be verified generally and implemented specifically for several technologically important semiconducting nanocrystal and nanocomposite systems. These include:

- (i) alkylamine-passivated photoluminescent InGaP, GaN, ZnSe, and ZnS nanocrystals, and
- (ii) electroluminescent conjugated polymer/inorganic nanocomposites, specifically blue-emitting poly(9,9-dioctylfluorenyl-2,7-diyl) (PFO), green-emitting poly(9,9-dioctylfluorenyl-2,7-diyl)-*co*-1,4-benzo-(2,1',3)-thiadiazole (F8BT), and red-emitting poly[2-methoxy-5(2'-ethyl-hexyloxy)-1,4-phenylene-vinylene] (MEH-PPV) incorporated into the nanostructured galleries of layered SnS<sub>2</sub> or cylindrical channels of block-copolymer-templated SiO<sub>2</sub>.

The application of very-high-field and multidimensional NMR characterization techniques have yielded unprecedented sensitivity and spectral resolution for these nanocrystal and nanocomposite systems that have provided enabling new insights on their molecular compositions, structures, and heterogeneous interfaces. These have been systematically analyzed with respect to materials synthesis/processing conditions and correlated with respect to the macroscopic photo- and electroluminescent properties and subsequent device performances of the respective nanocrystal and nanocomposite systems, including orientationally ordered systems. Notable new conclusions, insights, and discoveries follow for different project elements.

## Summary of Most Important Results

### *Indium gallium phosphide (InGaP) nanocrystals*

Photoluminescent (PL) properties of technologically important Group III-V semiconducting nanocrystals have been correlated with their surface and internal structures, which have been shown to depend on etching treatments and nanocrystal size. Compared to nanocrystalline Group II-VI compounds CdSe and CdS, Group III-V semiconductors, such as InP, GaP, InN, or GaN are less toxic, though have received less attention, in part because they have been available only as large, polydisperse particles. Advances in chemical synthesis protocols, however, have recently allowed the preparation of nanoscale Group III-V semiconductors and their ternary analogs (e.g., InGaP, InAlP) as monodisperse nanoparticles with discrete and tunable sizes. Their collective properties make them attractive alternatives to Cd-, Se-, and Te-based Group II-VI compounds for electrical, opto-electronic, or biological device applications.

Technologically important InGaP nanocrystals are especially complicated because of their ternary compositions and additional structural heterogeneities present. This is reflected in the PL quantum yields of as-synthesized ternary InGaP nanoparticles, which are modest, but which can be significantly enhanced by treating the particles with HF in methanol. For example, for 4.5 nm In<sub>0.91</sub>Ga<sub>0.09</sub>P nanoparticles in toluene, there is a dramatic increase in PL quantum efficiency from

<1% before HF treatment to ~50% afterward. After HF-treatment, the PL quantum yields of ternary  $\text{In}_{0.91}\text{Ga}_{0.09}\text{P}$  nanoparticles approach those sought for opto-electronic device applications, for which quantum efficiencies above 50% are typically required for commercial cost-effectiveness.

For the first time, the reasons for the enormous processing-dependent optical properties of Group III-V nanocrystals have been established as being due to a combination of size- and surface-dependent compositional and structural properties. Such insights were enabled by the first-ever solid-state  $^{71}\text{Ga}$  ( $I=3/2$ , 40% nat. abund., relative sensitivity 0.14 to  $^1\text{H}$ ) and  $^{115}\text{In}$  ( $I=9/2$ , 96% nat. abund., relative sensitivity 0.35) MAS NMR measurements acquired on Group III-V semiconductors. Studies on atomically ordered 4.5-nm [see Figure 1] and 6-nm  $\text{In}_{0.91}\text{Ga}_{0.09}\text{P}$  nanocrystals were conducted at very high magnetic field strengths (19.6 Tesla) during four separate visits to the National High Magnetic Field Laboratory in Tallahassee, Florida and carried out in collaboration with the group of Prof. Geoff Strouse in the Department of Chemistry at Florida State University.

Figure 2 shows  $^{71}\text{Ga}$  and  $^{115}\text{In}$  MAS spectra acquired at 19.6 T and under conditions of fast magic-angle-sample spinning at 25 kHz that display enormous improvements in  $^{71}\text{Ga}$  and  $^{115}\text{In}$  signal sensitivities and spectral resolution over that achievable using conventional conditions (11.7 T, 10 kHz MAS). For comparison, a spectrum of bulk polycrystalline  $^{71}\text{GaP}$  is shown in Figure 2(a), revealing a very narrow resonance at 302 ppm that is consistent with its expected highly uniform long-range order. This is in marked contrast to the broader and shifted  $^{71}\text{Ga}$  signals that are observed in Figure 2(b,c) for both as-synthesized and HF-etched  $\text{In}_{0.91}\text{Ga}_{0.09}\text{P}$  nanocrystals, which demonstrate unequivocally the existence of different  $^{71}\text{Ga}$  species that result from different processing treatments. The as-synthesized InGaP nanoparticles show broad peaks at ~200 ppm and -16 ppm, Fig. 2(b), the latter of which is similar to that measured separately for  $^{71}\text{Ga}_2\text{O}_3$  nanoparticles (not shown here). By comparison, upon etching the InGaP nanoparticles in hydrofluoric acid, significantly greater extents of local Ga site ordering are observed, as evidenced in Fig. 2(c) by the relatively narrow signal at -43 ppm near to that expected for gallo-oxophosphonate moieties. In combination with macroscopic photoluminescence measurements, these results establish that the formation of relatively ordered surface-oxide species, with fewer defects than the as-synthesized InGaP nanoparticles, play an important role in accounting for the significantly enhanced photoluminescent properties that the HF-etched nanocrystals display in solution.

The high field  $^{71}\text{Ga}$  measurements are consistent with separate  $^{115}\text{In}$  MAS spectra shown in Figure 3(a,b) also acquired at 19.6 T for the same as-synthesized and HF-etched InGaP samples as measured in Figures 1 and 2. The  $^{115}\text{In}$  MAS spectrum of the unetched InGaP nanocrystals [Fig. 3(a)] shows a very narrow line at 780 ppm prior to the etching treatment that is very similar to the signal observed for bulk polycrystalline InP powder at 780 ppm (not shown here.) By comparison, the  $^{115}\text{In}$  MAS spectrum acquired at 19.6 T for the HF-etched InGaP sample [Fig. 3(b)] shows a much broader resonance at approximately the same position, but reflecting a much broader distribution of  $^{115}\text{In}$  environments. These results point to InGaP nanoparticles having InP-rich cores and gallium oxide-rich peripheries.

Insights on the nature of the oxophosphonate species at the InGaP nanocrystal peripheries are established by powerful and complementary multidimensional solid-state  $^{31}\text{P}$  NMR measurements. As shown in Figure 4, two-dimensional (2D) Double-Quantum  $^{31}\text{P}\{^{31}\text{P}\}$  correlation spectra allow the relative proximities of surface  $\text{PO}_3$  and  $\text{PO}_4$  sites from each other at the nanocrystal surface to be established unambiguously. From the intensity correlations along the diagonal for the  $\text{PO}_4$  species, most of these moieties are determined to have other  $\text{PO}_4$  species as neighbors, while the absence of diagonal signal intensity for the  $\text{PO}_3$  moieties indicates that few if any other  $\text{PO}_3$  species are molecularly near (<1 nm). Nevertheless, appreciable off-diagonal signal intensity is shared between the  $\text{PO}_3$  and  $\text{PO}_4$  species, which establishes that nearly all of the  $\text{PO}_3$  moieties are surrounded by  $\text{PO}_4$  species. The structural implications of this with respect to nanocrystal shape [Fig. 1] and optical properties are still under investigation. These results demonstrate the powerful capabilities of such correlative molecular characterization methods and their utility for aiding nanocrystal-based

materials design strategies. The photoluminescence measurements correlated with the synthesis, etching and  $^{31}\text{P}$ ,  $^{71}\text{Ga}$  and  $^{115}\text{In}$  MAS NMR results acquired at 11.7 and 19.6 T allow the pronounced size-dependent optical properties of InGaP nanoparticles to be correlated with molecular differences in their heterogeneous surface and core compositions and structures. The increased understanding of InGaP nanocrystal properties at a molecular level are being used to facilitate their integration into host matrices and devices.

### ***ZnSe and ZnS nanowires and nanorods, ZnO***

Surfactant-passivated ZnSe and ZnS nanowires represent a closely related system with similar nanoscale composition/structural characterization issues and properties as the InGaP system described above. In cooperation with Prof. Yuval Golan and his group in the Department of Materials Engineering at Ben-Gurion University in Beer-Sheva, Israel, we have synthesized and characterized surfactant-passivated Group II-VI semiconductors ZnSe and ZnS nanowires and nanorods, with extremely high extents of local atomic ordering and adjustable direct-bandgap properties. Figure 5 shows representative high-resolution TEM images that, in conjunction with wide-angle XRD reflections, establish the high extents of local atomic positional order in these systems.

Such highly ordered atomic positions in these nano‘crystals’ might be expected to also possess high extents of local electronic order as well, but this is clearly not the case. Figure 6 shows much broader solid-state  $^{77}\text{Se}$  and  $^{67}\text{Zn}$  MAS signals than expected for a highly crystalline samples. Rather the  $^{77}\text{Se}$  ( $I=1/2$ , 7% nat. abund., relative sensitivity 0.00693) and  $^{67}\text{Zn}$  MAS ( $I=5/2$ , 4% nat. abund., relative sensitivity 0.0029) spectra in Figure 6 performed at 11.7 T and at 19.6 T, respectively, show linewidths that vary inversely with particle size for bulk polycrystalline ZnSe and different sizes of monodisperse ZnSe nanocrystals. These were exceedingly challenging measurements, due to the low natural abundances of both  $^{77}\text{Se}$  and  $^{67}\text{Zn}$ , long spin-lattice relaxation times of the  $^{77}\text{Se}$  nuclei and very weak gyromagnetic ratio and quadrupolar character of  $^{67}\text{Zn}$ . Nevertheless, the  $^{77}\text{Se}$  and  $^{67}\text{Zn}$  MAS spectra in Figure 6 show systematically much broader linewidths that increase inversely with shrinking nanocrystal size. Compared to the narrow (ca. 1 ppm wide)  $^{77}\text{Se}$  and  $^{67}\text{Zn}$  signals [Fig. 6(a)] for their cubic sites in bulk polycrystalline ZnSe (zincblende structure), the 10 and 5 nm ZnSe nanoparticles show signals [Fig. 6(b,c)] that retain partially bulk-like characters, but with a much broader distribution of local electronic environments. For the smallest 1.5 nm particles [Fig. 6(d)], in fact, no bulk-like signals are observed at all, rather only upfield-shifted resonances that are associated with distorted signals near the nanoparticle external peripheries. Fascinatingly, both the  $^{77}\text{Se}$  and  $^{67}\text{Zn}$  MAS spectra of the different nanoparticles show signals that appear to correspond to relatively ordered surface and/or near-surface sites that interact strongly with or are affected by the adsorbed passivating-surfactant species:  $^{77}\text{Se}$  signals at -380, -420, and -515 ppm and  $^{67}\text{Zn}$  signals at 335, 187, and 165 ppm. As for the InGaP nanoparticles described above, the extents of local electronic ordering in the nanoparticles, in addition to their sizes, both exert crucial and controllable influences on the macroscopic luminescence properties of these Group II-VI nanoscale semiconductors.

To exploit the novel and versatile properties of nanocrystals that are observed in solution, we are incorporating them into solid matrices to allow their integration into solid-state devices. By controlling carefully the rate of solvent evaporation, in conjunction with substrate selection, we have developed a protocol for preparing by soft-lithographic patterning micrometer channels in which host mesostructured silica/block-copolymer matrices can be highly aligned. As shown in Figure 7(a,b) scanning and focused ion-beam transmission electron microscopy, along with 2D small-angle X-ray scattering [Fig. 7(c)], show that over large regions of the patterned substrate, the hexagonal mesostructured silica nanocomposite channels are oriented vertically. Such aligned and patterned films provide anisotropic host matrices to incorporate the tunable nanocrystal systems discussed above into devices that will benefit from the resulting anisotropic optical opto-electronic, and/or

semiconducting properties. Specifically, 1.5 ZnS nanorods have been incorporated and orientationally ordered in hydrophobic-functionalized channels of aligned mesostructured silica and titania thin patterned films.

### ***Conjugated polymers in nanostructured composite materials***

A similar approach has been taken to characterize, understand, and optimize the properties of self-assembled on inorganic-conjugated polymer nanocomposites for solid-state light-emitting diodes (LEDs). In these systems, highly hydrophobic conjugated polymers are incorporated into nanostructured silica or chalcogenide host matrices, which impart crucial stability and device integrability to the opto-electronic component that is not possible to achieve otherwise. In collaboration with Dr. Gitti Frey (Dept. of Materials Engineering, Technion, Haifa, Israel), we have developed new means to understand, control, and optimize the processing of these materials to improve their light-emission properties, stabilities, and accompanying device performances. One technologically important example is the incorporation of blue-emitting poly-9,9-dioctylfluorene (PF8) into the galleries of layered inorganic chalcogenides, such as  $\text{SnS}_2$ . In this system, nanoscopic sheets of  $\text{SnS}_2$  are first delaminated by reaction of ion-exchanged Li cations with methanol, followed by reassembly of the  $\text{SnS}_2$  sheets in the presence of soluble conjugated polymers, such as PF8, also red-emitting poly[2-methoxy-5(2'-ethyl-hexyloxy)-1,4-phenylenevinylene] (MEH-PPV) or green-emitting poly(9,9-dioctylfluorenyl-2,7-diyl)-co-1,4-benzo-(2,1',3)-thiadiazole (F8BT). Resulting  $\text{SnS}_2$ /PF8 nanocomposites [Fig. 8(a)] emit in the blue region of the visible-light spectrum and, when incorporated into an LED device, exhibit dramatically enhanced stabilities, compared to conventional polymer LEDs. Figure 8(b) schematically depicts a solid-state 2D  $^{119}\text{Sn}\{^1\text{H}\}$  HETCOR MAS NMR experiment and accompanying 2D spectrum showing the transfer of polarization from nearby ( $< 1$  nm) hydrogenated polymer species to strongly interacting tin sites associated within the stabilizing and isolating  $\text{SnS}_2$  nanocomposite galleries. The strong and diverse intensity correlations that are attributed to the blue-emitting PF8 polymer species intercalated and isolated between the  $\text{SnS}_2$  sheets indicate strong interactions with multiple Sn surface sites in this sample prepared with deuterated solvent species. These 2D  $^{119}\text{Sn}\{^1\text{H}\}$  heteronuclear correlation experiments establish unambiguously the nature of these important interfacial interactions and their relationship to the optical properties observed. This information has allowed us to develop new non-aqueous routes for processing these technologically promising materials to achieve the key molecular features that lead to the optical performance properties sought.

Each of the nanocrystal and nanocomposite systems described above share similar daunting challenges to molecular characterization by any means, including NMR. Nevertheless, the uses of high magnetic field strengths, high MAS spinning rates, and multidimensional methods overcome many of the challenges of low sensitivity, heterogeneity, multicomponent complexity, and lack of long range order. Such state-of-the-art techniques are sensitive to interactions governed by local composition and structure in these materials, especially at interfaces and even in the absence of long-range order. In such cases as shown here, significant advancements in the fundamental understanding of technologically important semiconductor nanocrystal and nanocomposite solids are achieved with direct benefit to material and device improvements. Our advancements have benefited from close collaborative participation with several international research partners, who have provided important complementary expertises, especially with respect to material-property benchmarking and device integration. Resulting insights are being used to enable the development and integration of versatile, sensitive and robust nanocrystals and nanocomposites into devices of high technological interest to industry and the US Army, including as sensors, LEDs, opto-electronic devices, and for solid-state lighting.



## List of Publications

All papers, manuscripts, and invited lectures listed below relate directly to the synthesis and characterization of surfactant/polymer-templated nanocrystal, nanoparticle, and/or nanocomposite systems and acknowledge USARO funding support.

### Papers published in peer-reviewed journals:

S. Cadars, A. Lesage, B.F. Chmelka, L. Emsley, "Selective Measurements of Homonuclear Scalar Couplings in Isotopically Enriched Solids," *Journal of Physical Chemistry, B*, **110**, 16982-16991 (2006).

J.D. Epping, B.F. Chmelka, "Nucleation and Growth of Zeolites and Inorganic Mesoporous Solids: Molecular Insights from Magnetic Resonance Spectroscopy," *Current Opinions in Colloid and Interface Science*, **11**, 81-117 (2006).

E.S. Toberer, J.D. Epping, B.F. Chmelka, R. Seshadri, "Hierarchically Porous Rutile Titania: Harnessing Spontaneous Phase Changes in Mixed Metal Oxides," *Chem. Mater.*, **18**, 6345-6351 (2006).

### Manuscripts submitted and in preparation, but not yet published

M.G. Berrettini, C. Raab, J.D. Epping, J. Gerbec, G.F. Strouse, B.F. Chmelka, "Enhanced Optical Properties of Surface-Modified Monodisperse InGaP Nanoparticles," *Communication to the Journal of the American Chemical Society*, submitted.

S. Kirmayer, E. Dovgolevsky, M. Kalina, E. Lakin, J.D. Epping, B.F. Chmelka, G. L. Frey, "Self-Organized Mesostructured Silica Films from Non-Aqueous Solutions," *Chemistry of Materials*, submitted.

J.D. Epping, S. Cadars, N. Belman, S. Acharya, Y. Golan, B.F. Chmelka, "Electronic and Positional Order and Disorder in Monodisperse ZnSe Nanocrystals," *Physical Review Letters*, submitted.

J. Nolla, D. Wildemuth, G.L. Athens, C.A. Steinbeck, Y. Li, J. Lofvander, B.F. Chmelka, "Hierarchically Ordered Nano/Meso/Micropatterned Thin Films with Controllable Anisotropic Optical Properties," *Science*, manuscript in preparation.

J.D. Epping, A. Rapp, M.G. Berrettini, C. Raab, J. Gerbec, G.F. Strouse, B.F. Chmelka, "Compositional and Structural Heterogeneities in Photo-Luminescent InGaP Nanocrystals," *Journal of the American Chemical Society*, manuscript in preparation.

S. Cadars, J.D. Epping, N. Belman, S. Acharya, Y. Golan, B.F. Chmelka, "Size-Dependent Heterogeneities in Semi-Conducting ZnSe Nanocrystals," *Angewandte Chemie*, manuscript in preparation.

E. Aharon, M. Kalina, J.D. Epping, B.F. Chmelka, G. L. Frey, "White Electroluminescent Nanocomposites," *Journal of the American Chemical Society*, manuscript in preparation.

S. Bracco, A. Comotti, P. Sozzani, B.F. Chmelka, "Molecular dynamics in crystal-like pore walls of mesoporous organosilica," *Angewandte Chemie*, manuscript in preparation.

**Invited talks:**

American Institute of Chemical Engineers' National Meeting, San Francisco, Nov. 2006.  
Instituto de Investigaciones en Materiales, Universidad Nacional Autónoma de México, Mexico City, Nov., 2006.  
Department of Applied Surface Chemistry, Chalmers University, Göteborg, Sweden, September, 2006.  
Catalysis Summer Conference, PIRE-ECCI and International Center for Materials Research, UCSB, Aug., 2006.  
Porous Materials Summer School, International Center for Materials Research, UCSB, Aug., 2006.  
Centro de Investigación y Desarrollo, Network for Colloidal Systems, Barcelona, Spain, July, 2006.  
Departamento de Ingeniería Química, Universidad Rey Juan Carlos, Madrid, Spain, July, 2006.  
Nanotechnology Seminar, Ben Gurion University, Be'er Sheva, Israel, June, 2006.  
Nanoscience Seminar, Hebrew University, Jerusalem, Israel, May, 2006.  
Department of Chemistry, Weizmann Institute of Science, Rehovot, Israel, May, 2006.  
Department of Materials Engineering, Technion, Israel Institute of Technology, Haifa, April, 2006.  
Dow Chemical Company, New Materials Group, Midland, MI, December, 2005.  
Amberwave Technologies, Inc., Salem, NH, December, 2005.  
Department of Chemical and Biological Engineering, Chalmers University, Göteborg, Sweden, November, 2005.  
MRS Workshop on 3D Multifunctional Composites, Urbana-Champaign, Illinois, October, 2005.  
Department of Chemical Engineering, Iowa State University, Ames, Iowa, October, 2005.  
Department of Materials Science, Universita di Milano-Bicocca, Italy, September, 2005.  
Department of Chemistry, Universita di Udine, Italy, September, 2005.  
International Sol-Gel Society Symposium, Los Angeles, CA, August, 2005.  
7th Gambiaggi Winter School of Materials Physics, University of Buenos Aires, Argentina, July, 2005.  
Departamento de Ingeniería Química, Universidad Rey Juan Carlos, Madrid, Spain, June, 2005.  
European Materials Research Society, Layered Materials, Symposium E, Strasbourg, France, June, 2005.  
Experimental NMR Conference, Providence, RI, April, 2005.

**Awards:**

B.F. Chmelka, Meyerhoff Visiting Professor Award, Weizmann Institute of Science, Rehovot, Israel.  
B.F. Chmelka, 2006 Chalmers Jubilee Visiting Professor Award, Chalmers University, Goeteborg, Sweden.

**Invention disclosures, patents applied for and awarded:**

1 application pending.

B.F. Chmelka, J. Nolla, C.A. Steinbeck, G.L. Athens, "Patterned Inorganic Mesostructured Films Prepared with Controllable Orientational Ordering for Optical, Membrane, and Microfluidic Device Applications," U.S. patent application (UC06-477) filed November, 2006.

### **Transfer of materials or techniques to Army, DoD, or industry:**

The above pending UC patent is being licensed to AmberWave Technologies, Inc., Salem, NH for use in opto-electronic device and solid-state lighting development, with intention to license other patents that are expected to follow.

### **Value of this program to the Army**

In the present project, hierarchical control of opto-electronic material properties and devices has been achieved by controlling independently their compositions and structures over molecular, mesoscopic, micron, and/or macroscopic length scales. Novel synthesis and processing protocols have been developed that are based on new molecular understanding of dissimilar organic-inorganic and/or heterostructure semiconductor interfaces, which have for the first time been measured at a molecular level by using state-of-the-art methods of NMR spectroscopy. Progress has been enabled by the use of very-high field and multidimensional NMR, in conjunction with XRD, electron microscopy, and correlated with macroscopic material properties and device/process performances. This has lead to the development of new synthesis/processing strategies that provide unprecedented design flexibility and options for measuring and optimizing opto-electronic and optical material and device properties. These are enabling new applications in nano- and hierarchically structured sensors, integrated circuits, microfluidics/MEMS devices, and fuel cells.

### **List of Participating Scientific Personnel**

Professor Bradley F, Chmelka, principal investigator  
Dr. Jan Dirk Epping, post-doctoral researcher  
Dr. Sylvian Cadars, post-doctoral researcher  
Jordi Nolla, visiting PhD student, University of Barcelona

#### **Collaborating Research Groups:**

Professor Geoff Strouse, Dept. of Chemistry, Florida State University  
Professor Gitti Frey, Dept. of Materials Engineering, Technion Institute of Science, Israel  
Professor Yuval Golan, Dept. of Materials Engineering, Ben Gurion Univ., Israel  
Professor Piero Sozzani, Dept. of Materials Science, University of Milan, Italy

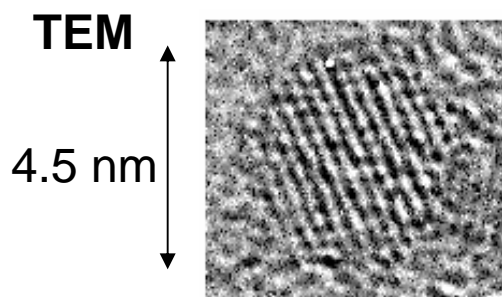


**Figure 1:** Transmission electron micrograph of a single as-synthesized 4.5 nm  $\text{In}_{0.91}\text{Ga}_{0.09}\text{P}$  nanocrystal passivated with hexadecylamine surfactant species.

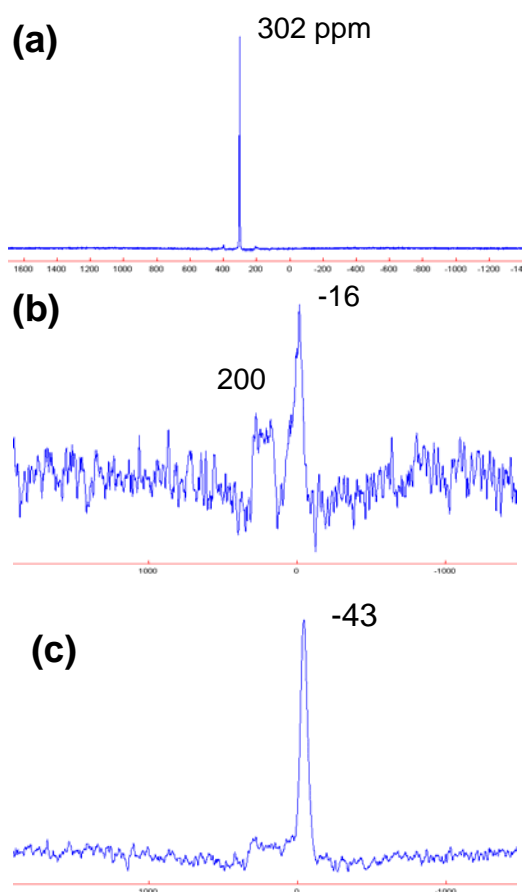


**Figure 2:** Solid-state  $^{71}\text{Ga}$  MAS NMR spectra acquired at 19.6 T and 25 kHz spinning speed of (a) bulk polycrystalline GaP, and 4.5 nm  $\text{In}_{0.91}\text{Ga}_{0.09}\text{P}$  nanoparticles (b) before and (c) after HF-etching.

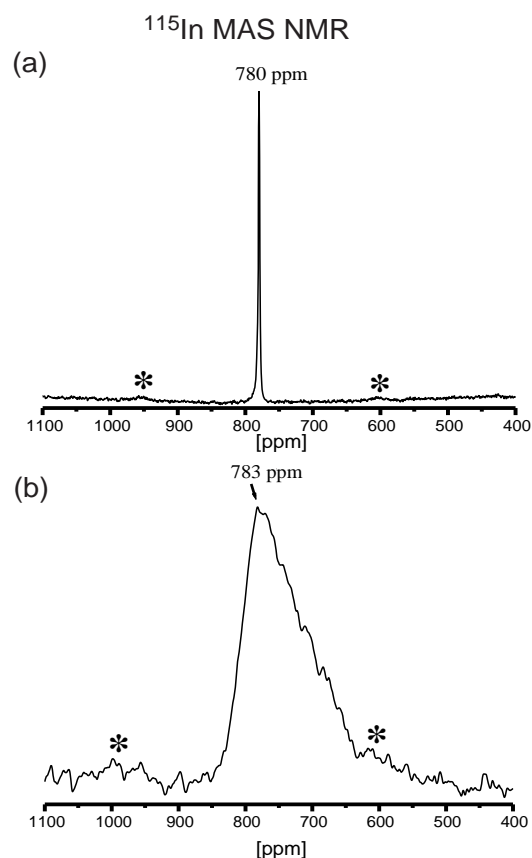


**Figure 3:** Solid-state  $^{115}\text{In}$  MAS spectra acquired at 19.6 T and an MAS spinning speed of 32 kHz of 4.5-nm  $\text{In}_{0.91}\text{Ga}_{0.09}\text{P}$  nanoparticles (a) before etching and (b) after etching with HF. (Bulk InP yields a  $^{115}\text{In}$  MAS peak at 780 ppm.)

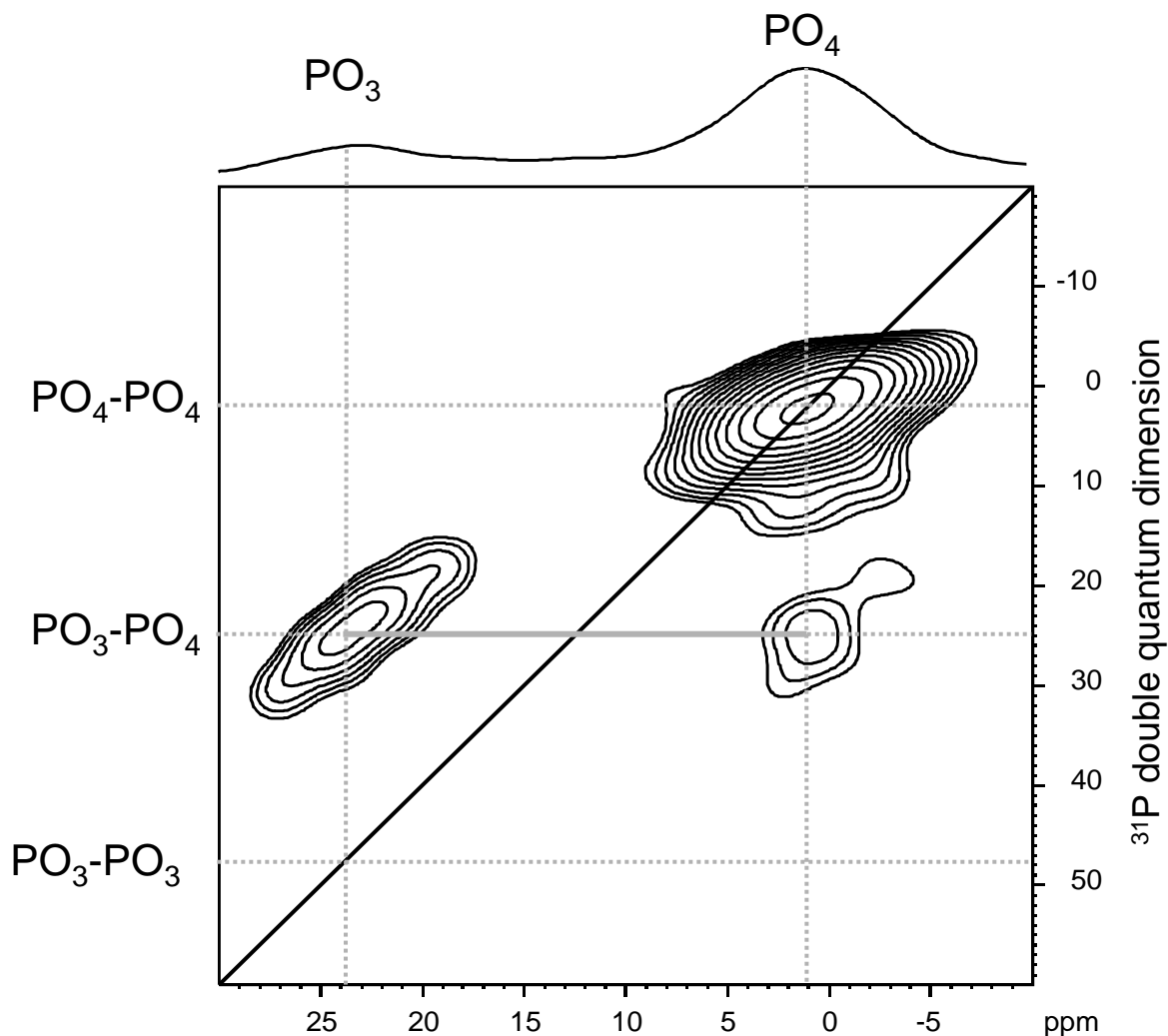


**Figure 4:** Solid-state 2D Double-Quantum  $^{31}\text{P}\{^{31}\text{P}\}$  NMR spectrum acquired at 11.7 T and 10 kHz MAS of 4.5 nm  $\text{In}_{0.91}\text{Ga}_{0.09}\text{P}$  nanocrystals shows molecularly near oxophosphorus moieties at near the particle peripheries. The intensity correlations establish dipole-dipole connectivities ( $<1$  nm) between  $\text{PO}_3\text{-PO}_4$  and  $\text{PO}_4\text{-PO}_4$  surface pairs, but no evidence for  $\text{PO}_3\text{-PO}_3$  species.

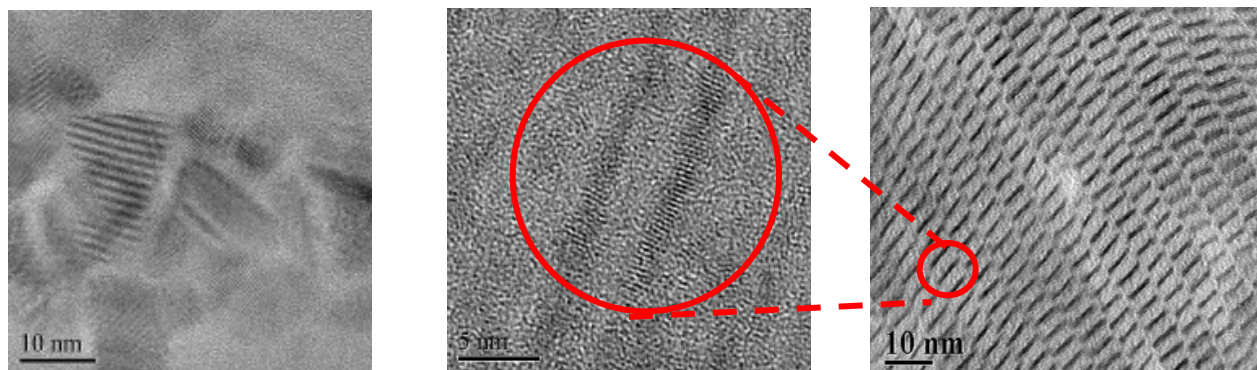


**Figure 5:** High-resolution transmission electron microscopy of ZnSe nanocrystals with mean diameters of (a) 10 nm, (b,c) 1.5 nm. Lattice fringes are clearly evident in (a) and (b), while (c) shows the high monodispersity of the 1.5 nm ZnSe nanocrystals. (Images courtesy of Y. Golan, BGU.)

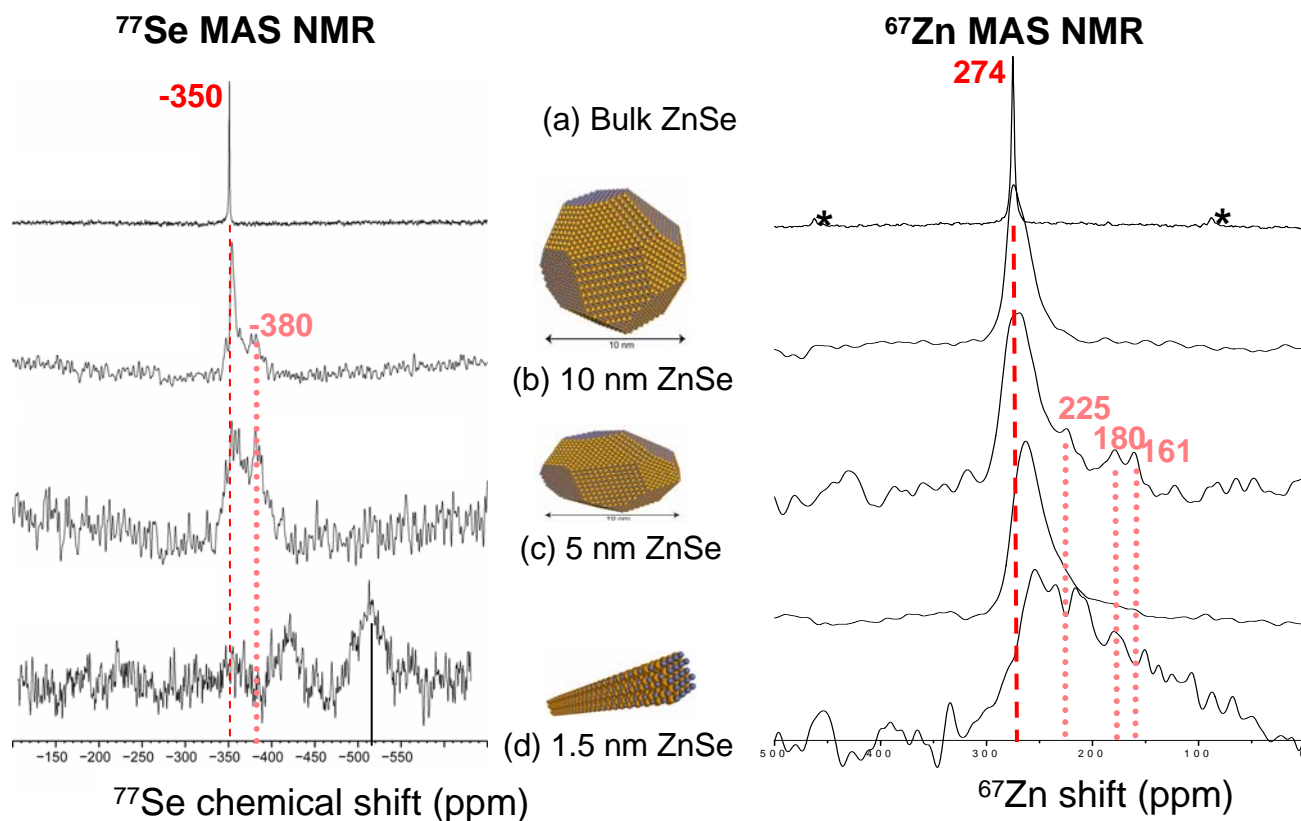
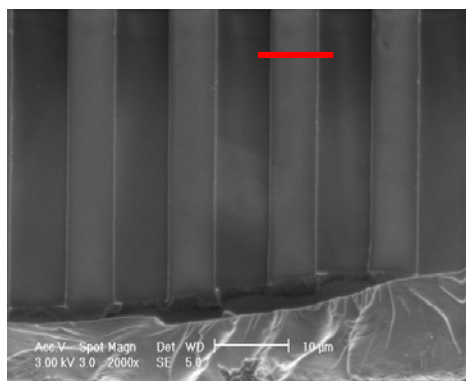


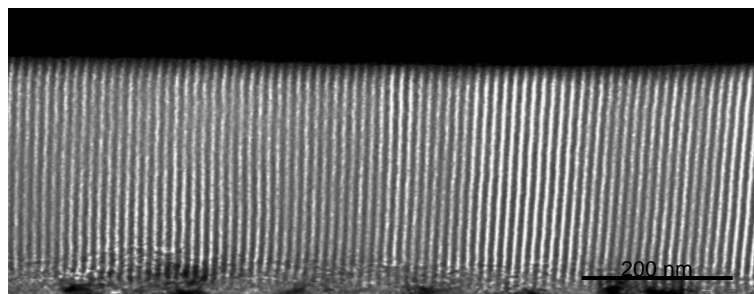
**Figure 6:** Solid-state  $^{77}\text{Se}$  and  $^{67}\text{Zn}$  MAS NMR spectra of (a) polycrystalline bulk ZnSe powder and ZnSe nanocrystals with mean diameters of (b) 10 nm, (c) 5 nm, and (d) 1.5 nm. Both the  $^{77}\text{Se}$  (acquired at 12 T) and the  $^{67}\text{Zn}$  spectra (acquired at 19.6 T) show dramatic evidence that near-surface  $^{77}\text{Se}$  and  $^{67}\text{Zn}$  sites experience broad distributions of local electronic environments, compared to bulk crystalline ZnSe, which contributes greatly to their measured luminescence properties.

(a) SEM



(b)

Focused Ion Beam TEM



(c) 2D transmission XRD

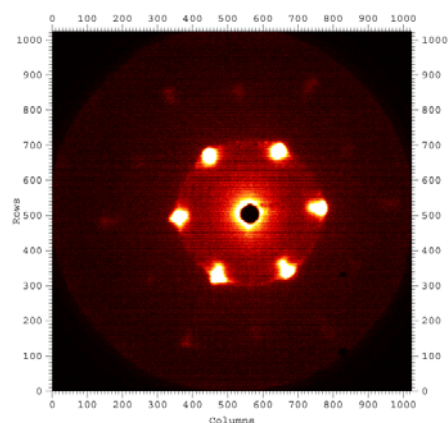
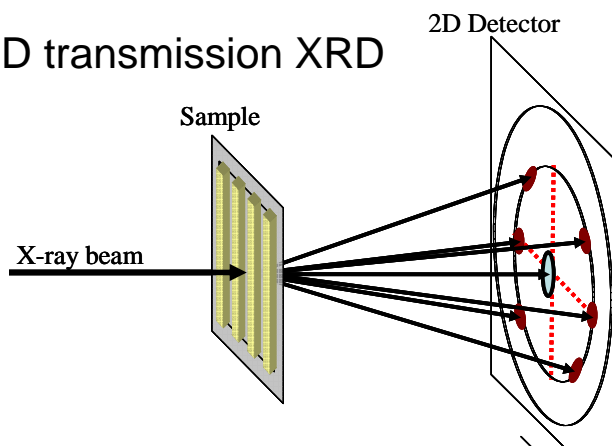


**Figure 7:** (a) Scanning electron micrograph of a soft-lithographically patterned mesostructured silica templated by block-copolymer species which yields an optically anisotropic host matrix for inclusion of aligned ZnSe, ZnS, and InGaP nanocrystals and conjugated polymer guest species. (b) Focused-ion-beam transmission electron micrograph showing the high extent of vertical alignment of the hexagonally ordered mesostructured silica host channels.

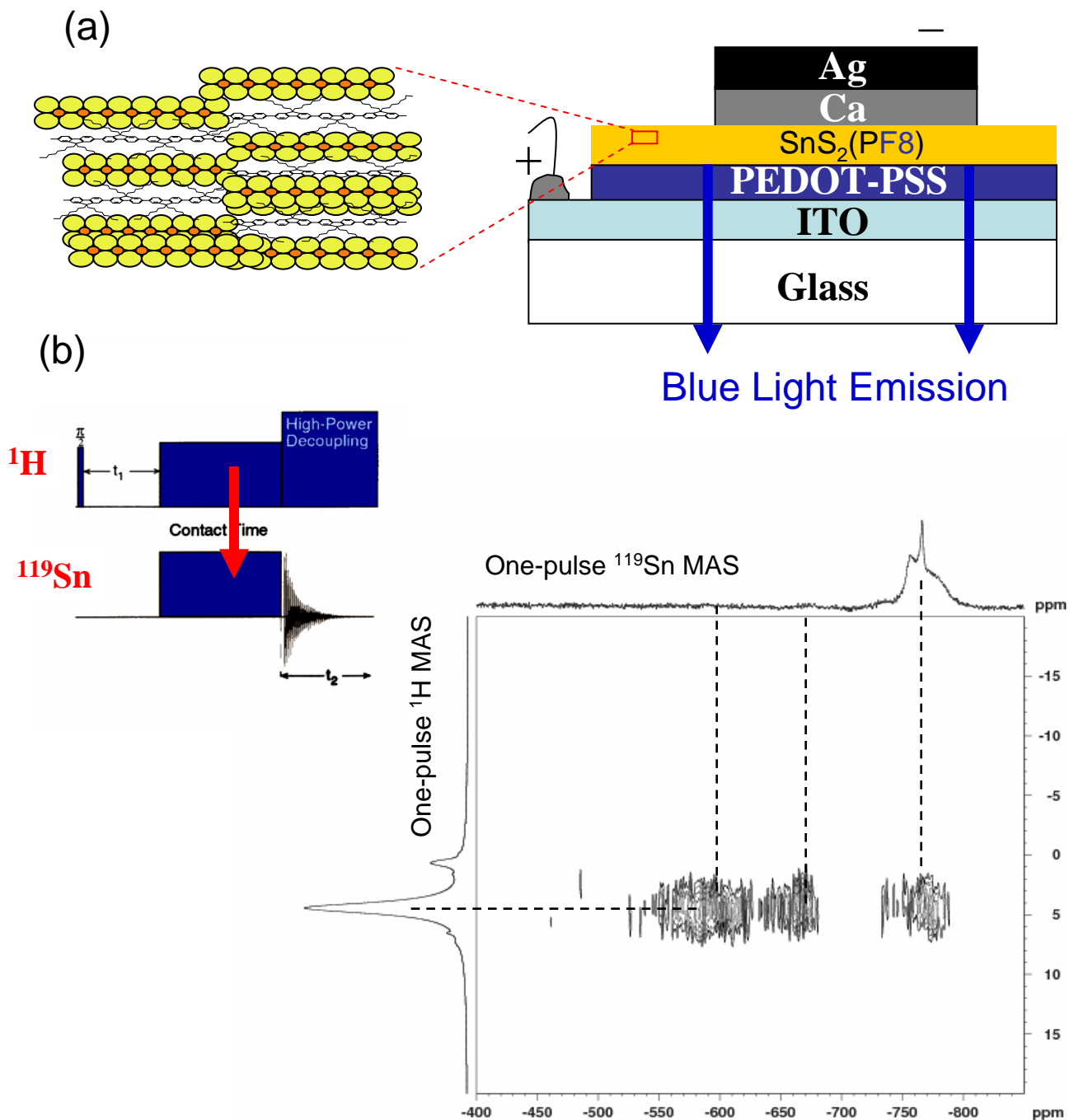


**Figure 8:** (a) PF8-intercalated  $\text{SnS}_2$  nanocomposite materials and solid-state device configuration for a blue light-emitting diode based (courtesy of G. Frey, Technion). (b) Solid-state 2D  $^{119}\text{Sn}\{^1\text{H}\}$  HETCOR MAS NMR experiment and spectrum acquired at 11.7 T and 10 kHz MAS for blue-emitting PF8-intercalated  $\text{SnS}_2$  prepared with deuterated solvent species and showing strong intensity correlations between the conjugated polymer and multiple surface Sn sites.